Journal of the Korean Electrochemical Society
Vol. 8, No. 2, 2005, 00-00

REVIEW

A Review of Ac-impedance Models for the Analysis of the Oxygen Reduction Reaction on the Porous Cathode Electrode for Solid Oxide Fuel Cell

Ju-Sik Kim and Su-Il Pyun†

Department of Materials Science and Engineering, Korea Advanced Institute of Science and Technology, 373-1 Guseong-Dong, Yuseong-Gu, Daejeon 305-701, Republic of Korea

(Received , 2005 : Accepted , 2005)

Abstract: This article covers the theoretical ac-impedance models for the analysis of oxygen reduction on the porous cathode electrode for solid oxide fuel cell (SOFC). Firstly, ac-impedance models were explained on the basis of the mechanism of oxygen reduction, which were classified into the rate-determining steps; (i) adsorption of oxygen atom on the electrode surface, (ii) diffusion of adsorbed oxygen atom along the electrode surface towards the three-phase (electrode/electrolyte/gas) boundaries, (iii) surface diffusion of adsorbed oxygen atom mixed with the adsorption reaction of oxygen atom on the electrode surface and (iv) diffusion of oxygen vacancy through the electrode coupled with the charge transfer reaction at the electrode/gas interface. In each section for ac-impedance model, the representative impedance plots and the interpretation of important parameters attributed to the oxygen reduction reaction were explained. Finally, we discussed in detail the applications of the proposed theoretical ac-impedance models to the real electrode of SOFC system.

Keywords: Solid oxide fuel cell, Adsorption, Diffusion impedance, Oxygen reduction, Ac-impedance spectroscopy.

1. Introduction

The overall losses in a solid oxide fuel cell are mainly controlled by the oxygen reduction reaction on the porous cathode electrode.[1)] In this respect, the mechanism of oxygen reduction on the porous cathode electrode has extensively been investigated by employing dc (direct current) potentiodynamic method and ac (alternating current) impedance spectroscopy,[2-8)] in order to minimise the overpotential caused by electrochemical cathodic reaction.

Especially, ac-impedance spectroscopy has widely been used to identify the various reaction steps and to determine the rate-determining step, since it provides an exceptionally powerful tool for separating the dynamics of several electrode processes with different relaxation times. In the analysis of their ac-impedance spectra measured on the porous cathode electrode, most researchers have employed the equivalent circuit simply described by a resistance and a capacitance.[9-11)] However, simple equivalent circuit composed of RC network does not give an adequate description of the ac response of the electrode, because the mechanism of oxygen reduction generally turns out to be much complicated in the real electrode system.[12,13)]

On the other hand, application of theoretical ac-impedance models for the analysis of oxygen reduction can not provide only an useful information on the general characteristic features of the shape of frequency dispersion, but also give a methods of extracting quantitative estimates of kinetic parameters from a straightforward analytical calculation of the measured impedance spectra.

Consequently, the present article considers the theoretical ac-impedance models for analysing of the oxygen reduction reaction on the porous cathode electrode. Firstly, all the proposed ac-impedance models were numerically derived from elementary reaction equations associated with the overall oxygen reduction reaction. Then, we discussed in details in each section about what ac responses are ascribed to kinetic processes that are rate-determining step for overall oxygen reduction. Finally, the proposed ac-impedance models were discussed for their application to the oxygen reduction reaction on the real porous cathode in SOFC system.

2. Various theoretical ac-impedance models for the oxygen reduction reaction

Now we consider some theoretical approach of impedance behaviour to the oxygen reduction reaction on the porous cathode electrode, which were classified into possible rate-determining steps.

2.1. Adsorption of oxygen atom on the electrode surface

Here we will theoretically present ac response of electrode, in case that the overall oxygen reduction reaction is purely controlled by adsorption of oxygen atom at electrode surface. If the adsorption reaction of oxygen atom is assumed to be a rate-determining step of cathodic reaction, the activity of oxygen atom in the adsorbed layer has approximately linear

†E-mail: sipyun@webmail.kaist.ac.kr

relationship with the quantity of adsorbed oxygen atom, so the electrode potential is fixed by the activity of oxygen atom O_{ad} in the adsorbed layer, obeying the Nernst equation as follows [14]:

$$E = \frac{RT}{2F}\ln c_{O_{ad}} \quad (1)$$

where E is the electrode potential, R the gas constant, T the absolute temperature, F the faradaic constant and $c_{O_{ad}}$ represents the concentration of oxygen atom in the adsorbed layer.

Accordingly, the electrode reaction is governed by the concentration of oxygen atom at electrode surface, and hence the overpotential of electrode is given as [14]:

$$\eta_{ad} = \frac{RT}{2F}\ln\frac{c_{O_{ad}}}{c^{eq}_{O_{ad}}} \quad (2)$$

where η_{ad} is the adsorption overpotential and $c^{eq}_{O_{ad}}$ denotes the adsorbed oxygen in equilibrium with the gas phase.

Under the assumption that adsorption process of oxygen atom proceeds dissociatively on the electrode surface, the equation of adsorption reaction is expressed as:

$$\frac{1}{2}O_{2,\,gas} = O_{ad} \quad (3)$$

The mass balance of adsorbed oxygen atom on the electrode surface is described by [14]:

$$\frac{\partial c_{O_{ad}}}{\partial t} = j_o + \frac{1}{2F} \quad (4)$$

$$\text{with } j_o = k_{ad}p_{O_2}^{1/2} - k_{des}c_{O_{ad}} \quad (5)$$

where t is the time, j_o the supplying rate of the overall oxygen from the gas to the adsorbed phase, I the current, p_{O_2} the oxygen partial pressure and k_{ad} and k_{des} denote the adsorption rate constant and the desorption rate constant, respectively.

From the differentiation of Eqs. (2) and (4) for small ac perturbations, the resulting impedance Z_{ad} [Ω] is finally obtained as [14]:

$$Z_{ad} = \frac{RT}{4F^2 c^s_{O_{ad}}}\frac{1}{(k_{ad} + j\omega)} \quad (6)$$

where $c^s_{O_{ad}}$ is the steady-state concentration of adsorbed oxygen atom.

From Eq. (5), the adsorption resistance R_{ad} [Ω] of electrode related to the oxygen concentration in the adsorbed layer is written by:

$$R_{ad} = \frac{RT}{4F^2 k_{ad} c^s_{O_{ad}}} \quad (7)$$

According to Eq. (6), it is suggested that the ac-impedance spectrum for the adsorption reaction of oxygen atom on the electrode surface exhibits simple one arc in shape. Fig. 1 shows the Nyquist plots of ac-impedance theoretically determined for adsorption of oxygen atom from Eq. (6) as a function of the rate constant k_{ad}, by assuming T=1273 K, $c^s_{O_{ad}} = 1 \times 10^{-4}$ mol cm^{-3}. All the simulated impedance spectra simply consist of an arc which decreases with increasing adsorption rate constant k_{ad}.

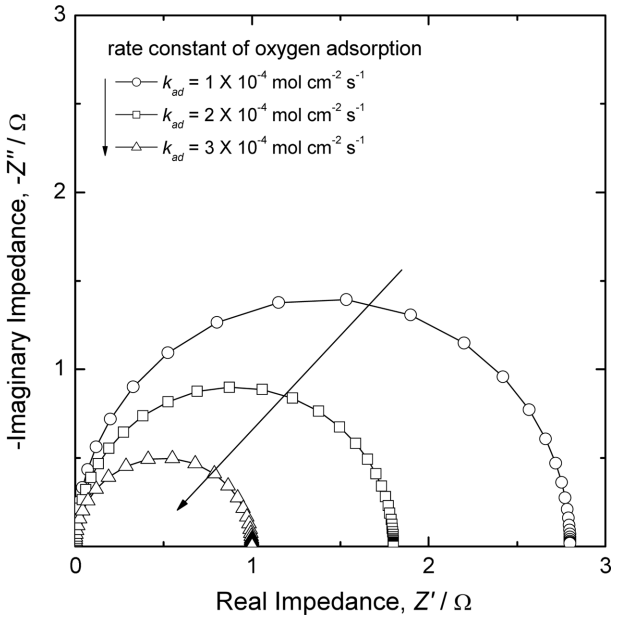

Fig. 1. Nyquist plots of the ac-impedance spectrum theoretically determined for adsorption of oxygen atom from Eq. (6) as a function of the adsorption rate constant k_{ad}. The values of the parameters involved in Eq. (6) were taken as T = 1273 K and = 1 × 10^{-4} mol cm^{-3}.

This model can account for the variation of adsorption resistance with the oxygen partial pressure, when oxygen reduction is purely determined by the adsorption reaction of oxygen atom at the electrode surface. Since the adsorption resistance is proportional to $1/c^s_{O_{ad}}$ according to Eq. (7), it can be inferred that the ac-impedance spectrum for the adsorption reaction has the dependence of from Eq. (3)

2.2. Diffusion of oxygen atom along the electrode surface towards the three-phase boundaries

For most cases of oxygen reduction on the porous cathode, many researchers have reported that the rate of cathodic performance is controlled by the diffusion of adsorbed oxygen atom along the electrode surface towards the electrochemical reaction sites the, i.e., three-phase boundaries (TPBs) among electrode, electrolyte and gas.[8,15,16] In order to deal with the problem of surface diffusion of oxygen atom, we will introduce the finite-length Warburg impedance model in this section.[17]

Fig. 2. illustrates the diffusion process of oxygen atom on the electrode surface. According to Fig. 2, overall oxygen reduction involves the following consecutive reaction steps: dissociative adsorption of oxygen atom on the electrode surface, followed by the charge transfer reaction at the TPBs which is represented as follows:

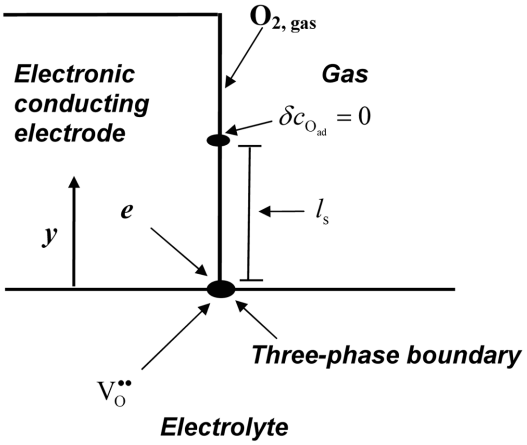

Fig. 2. Schematic diagram of the purely diffusion-controlled oxygen reduction. The diffusion of oxygen atom occurs along the electrode surface towards the three-phase boundaries. Here, is the oxygen vacancy,is the deviation of from the equilibrium concentration, *y* represents the distance from the electrode/electrolyte interface (*y*=0) towards bulk electrode and l_s denotes the average diffusion length.

$$\frac{1}{2}O_{2,\,gas} + 2e(electrode) + V_O^{\cdot\cdot}(electrolyte) = O_o(electrolyte) \quad (8)$$

In this case, the segment of electrode surface from the electrode/electrolyte interface is characterised by average diffusion length l_s [μm] along which the adsorbed oxygen atom diffuses to reach the TPBs. Furthermore, it is supposed to be no barrier preventing or slowing down the charge transfer reaction at the TPBs.

The diffusion behaviour of adsorbed oxygen atom at the electrode surface can be conveniently described by calculation of the one-dimensional diffusion equation as follows[17]:

$$\frac{\partial(\delta c_{O_{ad}})}{\partial t} = D_{S,\,O_{ad}} \frac{\partial^2(\delta c_{O_{ad}})}{\partial y^2} \quad (9)$$

where $\delta c_{O_{ad}}$ is the deviation of $c_{O_{ad}}$ from the equilibrium concentration, t is the diffusion time of adsorbed oxygen atom, y the distance from the electrode/electrolyte interface (y=0) towards bulk electrode and $D_{S,\,O_{ad}}$ represents the surface diffusivity of adsorbed oxygen atom. Therefore, average diffusion length l_s can be written as $2\sqrt{D_{S,\,O_{ad}}\tau_d}$.

Solving the Fick's diffusion equation of Eq. (9) under the semi-infinite boundary conditions of the oscillating concentration (or potential) perturbation at the electrode/electrolyte interface, diffusion impedance $Z_d(\omega)$ can be derived from Eq. (9) by using Laplace transform method as follows[17]:

$$Z_d(\omega) = \frac{RT}{4F^2 A_{ea} c^s_{O_{ad}} D_{S,\,O_{ad}}} \frac{\tanh(j\omega l_s^2 / D_{S,\,O_{ad}})^{1/2}}{(j\omega / D_{S,\,O_{ad}})^{1/2}} \quad (10)$$

where A_{ea} symbolises the electrode area, ω the angular frequency and j denotes the unit of the complex number $(\sqrt{-1})$. From Eq. (10), the diffusion resistance R_d [Ω] is taken per unit length:

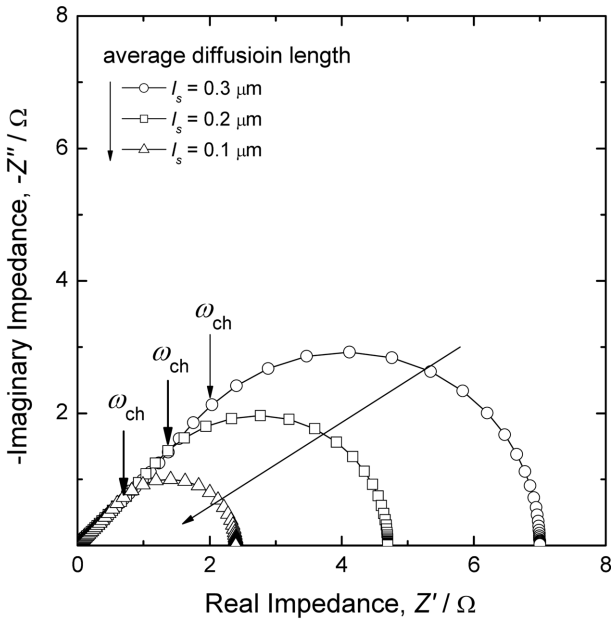

Fig. 3. Nyquist plots of the ac-impedance spectrum theoretically calculated for diffusion of oxygen atom at electrode surface from Eq. (10) as a function of average diffusion length l_s. The values of the parameters involved in Eq. (10) were taken as T = 1273 K, A_{ea} = 1 cm^2, = 1 × 10^{-1} mol cm^{-3},= 1.2 × 10^{-11} cm^2 s^{-1}.

$$R_{ad} = \frac{RTl_s}{4F^2 A_{ea} c^s_{O_{ad}} D_{S,\,O_{ad}}} \quad (11)$$

According to Eq. (10), the ac-impedance spectrum consists of a straight line inclined at a constant angle of 45° to the real axis in the high frequencies above the characteristic angular frequency $\omega_{ch} = 4D_{S,\,O_{ad}}/l_s^2$ but simple an arc in the low frequencies below $\omega_{ch} = 4D_{S,\,O_{ad}}/l_s^2$. This type of diffusion behaviour is commonly called the finite-length Warburg impedance.

Fig. 3 gives the typical ac-impedance spectra in Nyquist representation, theoretically calculated from Eq. (10) as a function of average diffusion length l_s, by assuming T=1273 K, A_{ea}=1 cm^2, $c^s_{O_{ad}}$=1×10^{-1} mol cm^{-3}, $D_{S,\,O_{ad}}$=1.2×10^{-11} cm^2 s^{-1}. In Fig. 3, it is found that the finite-length Warburg impedance strongly depends on the average diffusion length l_s but remains nearly constant in shape. From Figs. 1 and 2, one can readily distinguish in shape the impedance by diffusion of oxygen atoms from that impedance by adsorption of oxygen atoms.

2.3. Surface diffusion of oxygen atom mixed with the adsorption reaction of oxygen atom

It is frequently reported that overall oxygen reduction is not purely controlled by surface diffusion of adsorbed oxygen atom, but it is also affected by the slow adsorption reaction of oxygen atom.[13,18] Thus, rate-determining step for oxygen reduction can be explained in terms of the surface diffusion of oxygen atom coupled with adsorption process of oxygen

atom.[18)]

In this case, the impedance behaviour can be derived from the similar method as mentioned above in section ∮ 2.2. However, the adsorption reaction is coupled with the diffusion reaction on the electrode surface, so Fick's diffusion equation is modified by the adsorption reaction of oxygen atom as follows[18)]:

$$\frac{\partial(\delta c_{O_{ad}})}{\partial t} = D_{S,O_{ad}} \frac{\partial^2(\delta c_{O_{ad}})}{\partial y^2} + A_s(j_{ad} - j_{des}) \tag{12}$$

where A_s is the surface area of electrode per unit volume [cm^{-1}] and j_{ad} and j_{des} represent the adsorption and desorption flux of oxygen atom, respectively.

Assuming that the adsorption flux changes little from the equilibrium with small deviations, we obtain the total flux[18)]:

$$A_s(j_{ad} - j_{des}) = -\delta c_{O_{ad}} v_{ad} \exp\left(-\frac{E_{ad}}{RT}\right) = -\frac{\delta c_{O_{ad}}}{\tau_{ad}} \tag{13}$$

where v_{ad} represents the adsorption-desorption frequency [s^{-1}], E_{ad} the activation energy for the adsorption reaction and τ_{ad} denotes the mean life time [s] of oxygen atom in the adsorbed state.

Solving modified Fick's diffusion equation of Eq. (12) under semi-infinite boundary condition by using Laplace transform, one can obtain the following equation of $\delta c_{O_{ad}}$:

$$\delta c_{O_{ad}} = c_{O_{ad}} \exp\left\{-y\left[\frac{(j\omega + 1/\tau_{ad})}{D_{S,O_{ad}}}\right]^{1/2}\right\} \tag{14}$$

At the electrode/electrolyte interface (y=0), total electric current I [A] in the external circuit is expressed by the total flow of oxygen atom into the TPBs, considering the contribution of direct adsorption of oxygen atom from the gas phase into the TPBs[18)]:

$$I = -2F\left(D_{S,O_{ad}} + \frac{\partial(\delta c_{O_{ad}})}{\partial y} + f(j_{ad} - j_{des})\right) \text{ for } \quad y=0 \tag{15}$$

$$\text{with } \quad f = \frac{\lambda_{ad}}{\lambda_{TPB}} \tag{16}$$

where λ_{TPB} is the length of the three-phase boundaries (TPBs) per unit area [cm^{-1}] which means total reaction sites, λ_{ad} represents the effective length per unit area [cm^{-1}] for direct adsorption into the TPBs and f means the fraction of adsorption reaction current to the overall oxygen reduction current ($0 \le f \le 1$).

From Eqs. (14) and (15), we can derive the expression for the electrode impedance:

$$Z(\omega) = \frac{RT\lambda_{TPB}}{4F} \sqrt{\tau_{ad}/D_{S,O_{ad}}} \frac{1}{\lambda_{TPB}\sqrt{(1 + j\tau_{ad}\omega)} + r} \tag{17}$$

with characteristic length per unit area [cm^{-1}] for direct adsorption relative to diffusion,

$$r = \frac{f}{l_s} \tag{18}$$

$Z(\omega)$ representing Eq. (17) just corresponds to a Gerischer impedance[19)] parallel to a resistance $r(RT\lambda_{TPB}/4F^2 c^s_{O_{ad}}) \sqrt{\tau_{ad}/D_{S,O_{ad}}}$ [Ω]. r means the relative active adsorption length for the direct adsorption reaction to diffusion. If r=0, Eq. (17) is reduced to the Gerischer impedance. This indicates that the current for direct adsorption of oxygen atom into the TPBs is negligibly small.

Figs. 4(a) and (b) demonstrate the typical Nyquist plots of the ac-impedance spectrum theoretically determined for surface diffusion of oxygen atom mixed with adsorption of oxygen atom from Eq. (17) with (a) r=0 μm^{-1} and (b) r=10 μm^{-1} by assuming, $\lambda_{TPB}=5\times10^3$ cm^{-1}, $D_{S,O_{ad}} = 1.2\times10^{-11}$ cm^2 s^{-1}, $c^s_{O_{ad}}=1\times10^{-2}$ mol cm^{-3}, T=1273 K and τ_{ad}=0.1 s. The ac-

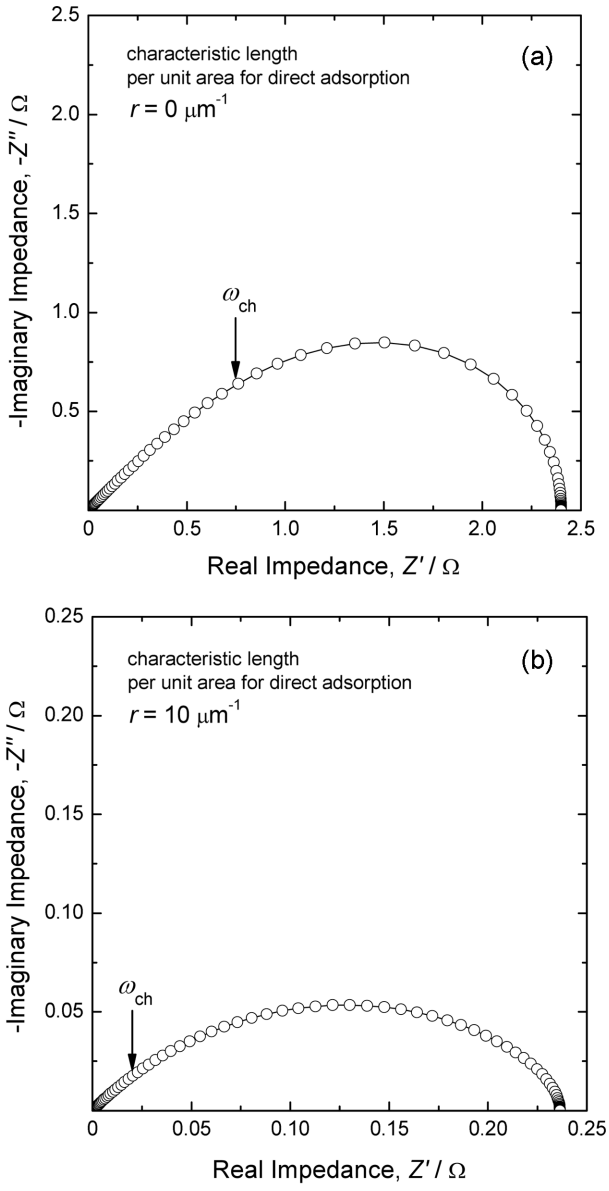

Fig. 4. Nyquist plots of the ac-impedance spectrum theoretically determined for surface diffusion of oxygen atom mixed with adsorption of oxygen atom from Eq. (17) with (a) r = 0 μm^{-1} and (b) r = 10 μm^{-1}. The values of the parameters involved in Eq. (17) were taken as $\lambda_{TPB}= 5\times10^3$ cm^{-1}, $= 1.2\times10^{-11}$ cm^2 s^{-1}, $= 1\times10^{-2}$ mol cm^{-3}, T = 1273 K and τ_{ad} = 0.1 s.

impedance spectrum computed with $r=0\ \mu m^{-1}$ exhibits clearly the Gerischer behaviour which is represented by a straight line making an constant angle of 45° to the real axis at high frequencies, followed by a simple arc at low frequencies. On the other hand, the ac-impedance spectrum simulated with $r=10\ \mu m^{-1}$ shows an asymmetric arc in shape. From this fact, it is strongly suggested that the characteristic length per unit area r for direct adsorption into the TPBs has an effect on the shape of frequency dispersion in the Nyquist plots.

The general expressions for the finite-length Warburg impedance $Z_F(\omega)$ and the Gerischer impedance $Z_G(\omega)$ are given as, respectively[19]:

$$Z_F(\omega) = Z_F^o \frac{\tanh(\sqrt{j\tau\omega})}{\sqrt{j\tau\omega}} \quad (19)$$

$$Z_G(\omega) = Z_G^o \frac{1}{\sqrt{(1+j\tau\omega)}} \quad (20)$$

where Z_F^o and Z_G^o represent the resistance of finite-length Warburg impedance and Gerischer impedance, respectively, and τ is the time constant. Under the semi-infinite diffusion boundary condition with permeable boundary condition, the finite-length Warburg impedance of Eq. (19) can be derived from Fick's diffusion equation, whereas the Gerischer impedance of Eq. (20) can be obtained from modified Fick's diffusion equation for the participation of another reaction.

Fig. 5 shows the discrepancy of the finite-length Warburg impedance and the Gerischer impedance, theoretically calculated from Eqs. (19) and (20), respectively, by assuming $Z_F^o = 2.4\ \Omega$, $Z_G^o = 2.4\ \Omega$ and $\tau = 0.1$ s. In high frequency ranges, both of impedance spectrum show semi-infinite diffusion behaviour as well, but in the low frequency ranges, the frequency dispersions are distinctly different.

The one of the plausible reasons for this discrepancy of low frequency dispersions is that the Gerischer impedance represents definitely a finite dc resistance associated with additional electrochemical process in the low frequency ranges, in contrast to the finite-length Warburg impedance. The remarkable point about the Gerischer impedance is that another frequency dispersion appears in low frequency ranges. Thus, for the diffusion reaction in combination with the adsorption reaction, the occurrence of the Gerischer impedance can easily be explained.

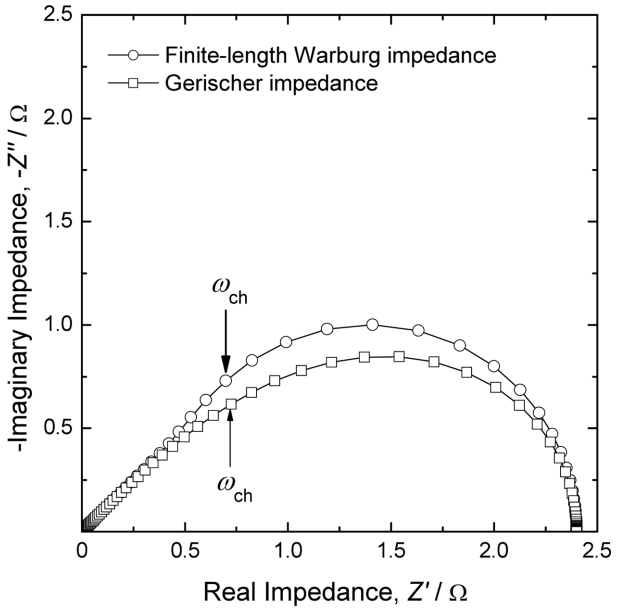

Fig. 5. Nyquist plots of the ac-impedance spectrum theoretically calculated for the general finite-length Warburg impedance and the Gerischer impedance from Eqs. (19) and (20). The values of the parameters involved in Eqs. (19) and (20) were taken as=2.4 Ω , = 2.4 Ω and *t* = 0.1 s

2.4. Bulk diffusion of oxygen vacancy mixed with the charge transfer reaction at the electrode/gas interface.

Let us consider the oxygen reduction reaction on the mixed conductor which holds generally the high concentration of oxygen vacancy[20,21]. The mechanism of oxygen reduction on the mixed conductor is visualised in Fig. 6. In contrast to the case of electronic conductor, it can tentatively be expected that the overall oxygen reduction reaction on the mixed conducting electrode is split into the following two consecutive substeps: diffusion of oxygen vacancy through the electrode and subsequent electron exchange reaction between oxygen vacancies and gaseous oxygen (charge transfer reaction) at the electrode/gas interface.

According to Fig. 6, it can be deduced that oxygen reduction is not restricted to the TPBs, but it is significantly extended from the origin of the TPBs into the electrode/gas interface segments as far as the extended electrochemical reaction length l_{EPB} [μm]. In contrast to Eq. (8), the charge transfer reaction at the electrode/gas interface is written as:

$$\frac{1}{2}O_{2,\,gas} + 2e(electrode) + V_O^{\cdot\cdot}(electrolyte) = O_o(electrolyte) \quad (21)$$

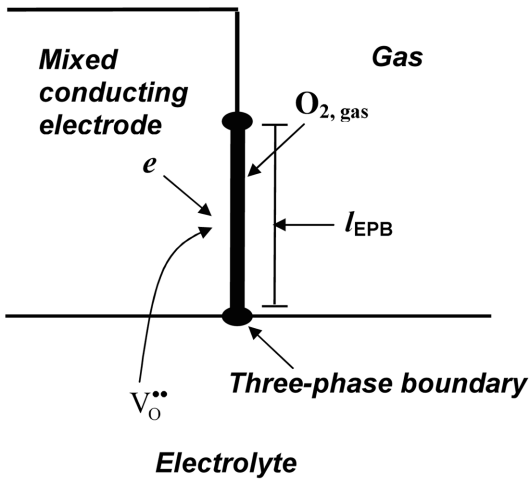

Fig. 6. Schematic diagram of the diffusion reaction of oxygen vacancy mixed with charge transfer reaction at the electrode/gas interface for mixed conducting electrode. l_{EPB} represents the extended active reaction length.

At this point, we will introduce an impedance model for oxygen reduction on the mixed conductor developed by Adler et al.[22]. The governing equation for oxygen vacancy transport through the electrode is given as the modified Fick's diffusion equation as follows[22]:

$$(1-\varepsilon)\frac{\partial(\delta c_{V_o^{\cdot\cdot}})}{\partial t} = \left(\frac{1-\varepsilon}{\tau_p}\right) W_{th} D_{V_o^{\cdot\cdot}} \frac{\partial^2(\delta c_{V_o^{\cdot\cdot}})}{\partial y^2} - A_s j_{\text{int}} \tag{22}$$

with the instantaneous exchange flux j_{int} at the electrode/gas interface,

$$j_{\text{int}} = j_e \left\{ \exp\left(\frac{\alpha_1}{RT}\Delta\mu_{\text{int}}\right) - \exp\left(-\frac{(1-\alpha_1)}{RT}\Delta\mu_{\text{int}}\right) \right\} \tag{23}$$

where $c_{V_o^{\cdot\cdot}}$ is the oxygen vacancy concentration in the electrode, $\delta c_{V_o^{\cdot\cdot}}$ the deviation of $c_{V_o^{\cdot\cdot}}$ from the initial concentration, t the diffusion time of oxygen vacancy, ε the porosity of electrode, τ_p the pore tortuosity of electrode, W_{th} the thermodynamic enhancement factor of the diffusivity of oxygen vacancy, $D_{V_o^{\cdot\cdot}}$ the component diffusivity of oxygen vacancy, j_o the equilibrium exchange flux at $t=\infty$, α_1 the transfer coefficient for oxygen absorption, $\Delta\mu_{\text{int}}$ the difference between the chemical potentials of oxygen vacancies in the electrode and gaseous oxygen and R represents the gas constant.

Solving the modified Fick's diffusion equation of Eq. (20) under the boundary conditions of the oscillating concentration (or potential) perturbation at the electrode/electrolyte interface (y=0) and of the semi-infinite diffusion of oxygen vacancy, the following expression for $\delta c_{V_o^{\cdot\cdot}}$ is obtained[22]:

$$\delta c_{V_o^{\cdot\cdot}} = \frac{E_o F c_{V_o^{\cdot\cdot}}}{W_{th} RT} \exp\left(-\frac{y}{l_{EPB}}\sqrt{1-j\omega t_{ch}} - j\omega t_{ch}\right) \tag{24}$$

$$\text{with } t_{ch} = \frac{c_{V_o^{\cdot\cdot}}(1-\varepsilon)}{W_{th} A_s j_e} \tag{25}$$

$$\text{and } l_{EPB} = \sqrt{\frac{c_{V_o^{\cdot\cdot}} D_{V_o^{\cdot\cdot}} (1-\varepsilon)}{\tau_p A_s j_e}} \tag{26}$$

where E_o is the ac-amplitude of the oscillating potential, ω is the angular frequency, and t_{ch} denotes in a first approximation the characteristic time constant required for diffusion of oxygen vacancy from the electrode/gas interface through the electrode to the electrode/electrolyte interface. In addition, l_{EPB} represents the distance at which the value of drops to (1/e) of the value at y=0 at steady-state (t=°f, ω=0), and thus it is usually taken as the extended active reaction length which can be understood by the amount of two-dimensionally extended TPBs length λ_{TPB} towards the bulk electrode.

The electric current I [A] at the electrode/electrolyte interface is expressed by

$$I = -\frac{2F(1-\varepsilon)}{\tau_p} W_{th} D_{V_o^{\cdot\cdot}} \frac{\partial(\delta c_{V_o^{\cdot\cdot}})}{\partial y} \quad \text{for} \quad y = 0 \tag{27}$$

From Eqs. (22) to (25), the electrode impedance $Z(\omega)$ is finally given as

$$Z(\omega) = R_{ch}\sqrt{\frac{1}{1+j\omega t_{ch}}} \tag{28}$$

$$\text{with } R_{ch} = \left(\frac{RT}{2F^2}\right)\sqrt{\frac{\tau_p}{(1-\varepsilon)c_{V_o^{\cdot\cdot}} D_{V_o^{\cdot\cdot}} A_s j_e}} \tag{29}$$

where R_{ch} designates the characteristic resistance [Ωcm^2] for the oxygen reduction reaction.

Fig. 7 depicts the Nyquist plots of the ac-impedance spectrum theoretically determined for bulk diffusion of oxygen atom mixed with the charge transfer reaction at the electrode/gas interface from Eq. (28), by assuming, T = 1273 K, τ_p = 2.5, ε = 0.3, $c_{V_o^{\cdot\cdot}} = 1.8\times10^{-3}$ mol cm^{-3}, $D_{V_o^{\cdot\cdot}} = 1\times10^{-5}$ cm^2 s^{-1}, A_s = 1.5 cm^{-1}, j_e=5.5×10^{-6} mol cm^{-2} s^{-1} and t_{ch} = 0.1 s. In Fig. 7, the ac-impedance spectrum clearly displays the Gerischer behaviour which is exactly the same as the impedance behaviour in Fig. 4(a).

As already pointed out in preceding section §2.3, the Gerischer impedance of Eq. (28) reflects the diffusion process mixed with another electrochemical reaction which can be regarded as the charge transfer reaction in the case of oxygen reduction on mixed conducting electrode. In consideration of the diffusivity of oxygen vacancy and the equilibrium exchange flux evaluated from this impedance model, the mechanism of oxygen reduction can be analysed[22,23]. In summary, the Gerischer impedance is embodied in two forms: one involves surface diffusion of oxygen atoms coupled with adsorption apart from direct adsorption already shown in Fig.

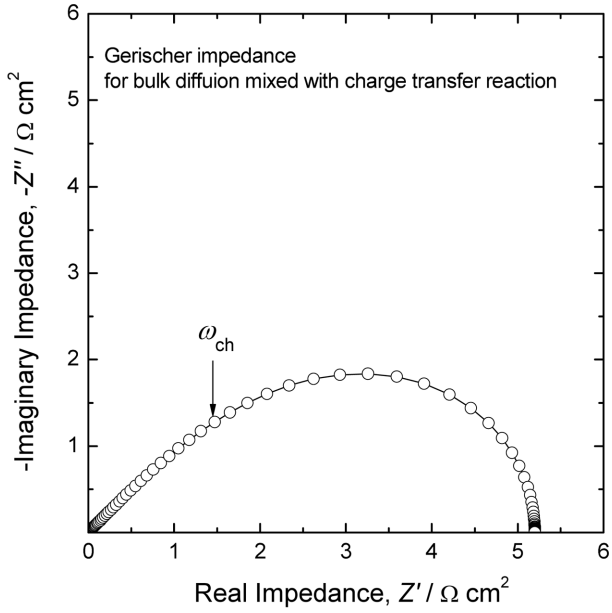

Fig. 7. Nyquist plots of the ac-impedance spectrum theoretically determined for bulk diffusion of oxygen vacancy mixed with charge transfer reaction at the electrode/gas interface from Eq. (28). The values of the parameters involved in Eq. (28) were taken as T = 1273 K, τ_p=2.5, ε = 0.3, = 1.8 × 10^{-3} mol cm^{-3}, =1 × 10^{-5} cm^2 s^{-1}, A_s= 1.5 cm^{-1}, = 5.5 × 10^{-6} mol cm^{-2} s^{-1} and t_{ch} = 0.1 s.

4(a), the other establishes bulk diffusion coupled with the charge transfer reaction already represented by Fig. 7.

3. Discussion about the application of ac impedance models to real electrode system.

Many researchers have recently attempted to apply these impedance models to the interpretation of the oxygen reduction reaction on the cathodic electrode for solid oxide fuel cell[8,14,17,18]. The mechanism of oxygen reduction can be inferred from the comparison the measured impedance spectra with the results of impedance based upon the various theoretical impedance models. Furthermore, one can quantitatively analyse the kinetic parameters for cathode performance obtained from the proposed ac-impedance models[22,23].

However, the measured impedance spectra are very sensitive to test circumstances and the electrode performance is influenced by the previous electrochemical history and intrinsic kinetic and thermodynamic properties of cathode electrode, so those complexity limits the ability of the model to represent accurately the measured impedance data[24]. Thus, in order to increase the credibility of ac-impedance models, it is of great importance to consider the important factors governing the cathodic performance. In this respect, before applying the ac-impedance models to the electrode reaction, it is necessary to obtain the information for electrical and geometrical properties of the electrode.

3.1. Electronic conducting electrode system

For the noble metal electrode such as Pt, Ag and peroveskite oxide electrode such as Sr-doped $LaMnO_3$ which are generally regarded as an electronic conductor, the diffusion of oxygen vacancy through the electrode can be assumed to be negligible for the oxygen reduction reaction due to their very low concentration of oxygen vacancy[25,26]. In this case, the overall oxygen reduction reaction proceeds only at the TPBs as shown in Fig. 2. Consequently, the impedance models, which were proposed in section §2.1 to §2.3, can be applied to the investigation of oxygen reduction on the electronic conducting cathodes.

Let us now discuss the application of ac-impedance models to an electronic conductor. Siebert et al. [14] have investigated the oxygen reduction on the $La_{0.8}Sr_{0.2}MnO_3$ electrode by using the theoretical ac-impedance model for the adsorption reaction as mentioned in section §2.1. It was deduced that the impedance arc is associated with the adsorption reaction, because it shows the dependence on $p_{O_2}^{-1/2}$.

Iori et al.[27] reported that the ac-impedance spectra measured on the porous $La_{0.85}Sr_{0.15}MnO_3$ electrode is ascribed to surface diffusion of oxygen atom, since it is well fitted to the finite-length Warburg impedance. Matsuzaki and Yasuda[6] verified that this finite-length Warburg impedance is adequate for analysing the low frequency arc measured on the $La_{0.6}Sr_{0.4}MnO_3$ electrode, making clear the relationship between the cathodic limiting current density and impedance fitting data. Although the impedance spectra did not exactly follow in shape the finite-length Warburg impedance, the measured impedance spectra may give the results for surface diffusion of oxygen atom overlapped with another reactions such as adsorption reaction and charge transfer reaction in the high frequency ranges[28,29].

Braunshtein et al.[29] and Sasaki et al.[30] have attempted to illustrate the ac-impedance spectra obtained from Pt electrode on the basis of surface diffusion of oxygen atom mixed with adsorption of oxygen atom. In these papers, according to the model addressed in section §2.3, it was demonstrated that the measured ac-impedance spectra deviated in shape from ideal Gerischer behaviour because of the addition of slow direct adsorption reaction to the diffusion reaction of oxygen atom.

3.2. Mixed conducting electrode system

For electronic/ionic mixed conductors with high concentration of oxygen vacancy, we can expect that impedance spectra follow the Gerischer behaviour, since the oxygen reduction reaction involves diffusion of oxygen vacancy through the electrode as shown in Fig. 6. In practice, it was found that the ac-impedance spectrum on those intrinsic mixed conductors such as $La_{0.6}Sr_{0.4}CoO_3$[31] and $(La_{0.6}Sr_{0.4})(Co_{0.2}Fe_{0.8})O_3$[21] shows the Gerischer impedance. Adler[31] has investigated the important kinetic parameters associated with oxygen reduction on the porous $La_{0.6}Sr_{0.4}CoO_3$ electrode, employing the impedance model for mixed conductor suggested in section §2.4

It was also observed that the ac-impedance spectrum measured on the porous $(La_{0.85}Sr_{0.15})_{0.9}MnO_3$ electrode subjected to the cathodic polarisation is quite similar in shape to the Gerischer impedance, which justifies the theoretical ac-impedance model for the mixed conducting cathode in which the rate of the overall oxygen reduction is determined by the mixed control of the charge transfer reaction and the subsequent oxygen vacancy diffusion[23].

3.3. Suggestions for the advanced impedance model

As a matter of fact, it is usually found that the ac-impedance spectrum on a porous cathodic electrode does not fairly coincide in shape with the results of impedance spectrum simulated based upon theoretical ac-impedance models[1,24,32]. This inconsistence can be interpreted as the complexity of the real situation. In other words, all the proposed ac-impedance models are assumed to be one-dimensional reaction and macro-homogeneous electrode, so the relationship between electrode performance and the microstructure of electrode is disregarded in the impedance model. Oxygen reduction depends on the electrode composition as well as on the microstructure. Impurities and secondary phases may inhibit the electrode kinetics, leading to inhomogeneity of active reaction sites and uneven distribution of kinetic parameters such as diffusivity and rate constant, etc. Furthermore, electrode composition and microstructure can hardly be specified or controlled, since electrode performance changes with time, temperature, thermal cycle, operating conditions.

Thus, it is necessary to modify ac-impedance model on various assumptions about the real porous electrode system, by effectively considering the complicated circumstances on the porous cathodic electrode, in order to draw meaningful

conclusions from the ac-impedance models.

3. Concluding remarks

The present article provided the overview of the theoretical ac-impedance models for oxygen reduction on the porous cathodic electrode. All the ac-impedance models were numerically treated in terms of rate-determining steps for oxygen reduction, and then we explained the characteristic features attributed to the shape of ac-impedance spectrum and the important parameters associated with oxygen reduction. Finally, we discussed in detail the application of the proposed ac-impedance models to investigation of oxygen reduction on the real porous cathode in SOFC system.

From the results of this article, it is recognised that the theoretical ac-impedance model can effectively provide an useful information to reveal the mechanism of oxygen reduction on the porous cathode and to evaluate such kinetic parameters as rate constant, diffusivity and exchange current, etc. However, unfortunately, it is usually difficult to correlate the measured impedance arcs to specific impedance model, because the real electrode system is very complex and the elementary reactions with similar relaxation time can simultaneously be present in the overall oxygen reaction. Therefore, in order to increase the credibility and usefulness of the proposed ac-impedance models, it is needed the deep comprehension of electrode system and the modification of theoretical ac-impedance model for the real situation.

Acknowledgements

The receipt of a research grant No. N-FC12-P-03-3-010 for 5-year period 2004/2009 from Korea Energy Management Corporation is gratefully acknowledged. Furthermore, this work was partly supported by the Brain Korea 21 project.

Nomenclature

A_{ea}	electrode area (cm^2)
A_s	surface area per unit volume (cm^{-1})
α_1	transfer coefficient for oxygen absorption
$c_{O_{ad}}$	concentration of oxygen atom in the adsorbed layer (mol cm^{-3})
$c^{eq}_{O_{ad}}$	concentration of adsorbed oxygen in equilibrium with the gas phase (mol cm^{-3})
$c^{s}_{O_{ad}}$	steady-state concentration of adsorbed oxygen atom (mol cm^{-3})
$c_{V_o^{\cdot\cdot}}$	oxygen vacancy concentration in the electrode (mol cm^{-3})
$D_{S,O_{ad}}$	surface diffusivity of adsorbed oxygen atom (cm^2 s^{-1})
$D_{V_o^{\cdot\cdot}}$	component diffusivity of oxygen vacancy (cm^2 s^{-1})
E	electrode potential (V)
E_{ad}	activation energy for the adsorption reaction (J mol^{-1})
E_o	ac-amplitude of the oscillating potential (V)
ε	porosity of electrode
F	faradaic constant (C mol^{-1})
f	fraction of the adsorption reaction current to the overall oxygen reduction current
I	current (A)
j	unit of the complex number ($\sqrt{-1}$)
j_e	equilibrium exchange flux at $t=\infty$ (mol cm^{-2} s^{-1})
j_o	supplying rate of the overall oxygen from the gas to the adsorbed phase (mol cm^{-2} s^{-1})
j_{ad}	adsorption flux of oxygen atom (mol cm^{-2} s^{-1})
j_{des}	desorption flux of oxygen atom (mol cm^{-2} s^{-1})
k_{ad}	adsorption rate constant (mol s cm^{-3})
k_{des}	desorption rate constant (mol s cm^{-3})
l_s	average diffusion length (μm)
l_{EPB}	extended active reaction length (μm)
λ_{ad}	effective length per unit area for direct adsorption into the TPBs (cm^{-1})
λ_{TPB}	length of three-phase boundaries per unit area (cm^{-1})
$\Delta\mu_{int}$	difference between the chemical potentials of oxygen vacancies in the electrode and gaseous oxygen (J mol^{-1})
p_{O_2}	oxygen partial pressure (atm)
r	relative active adsorption length for the direct adsorption reaction to diffusion
R	gas constant (J mol^{-1} K^{-1})
R_{ad}	adsorption resistance (Ω)
R_{ch}	characteristic resistance (Ω cm^2)
R_d	diffusion resistance (Ω)
T	absolute temperature (K)
t	time (s)
t_{ch}	characteristic time constant required for diffusion of oxygen vacancy from the electrode/gas interface through the electrode to the electrode/electrolyte interface (s), $t_{ch} = 2\pi/\omega_{ch}$
τ	time constant (s)
τ_a	mean life time of oxygen atom in the adsorbed state (s)
τ_p	pore tortuosity of electrode
η_{ad}	adsorption overpotential (V)
$V_o^{\cdot\cdot}$	oxygen vacancy
W_{th}	thermodynamic enhancement factor of the component diffusivity of oxygen vacancy
ω	angular frequency (rad s^{-1})
ω_{ch}	characteristic angular frequency (rad s^{-1}), $\omega_{ch}=2\pi/t_{ch}$
y	distance from the electrode/electrolyte interface (y=0) towards bulk electrode (μm)
v_{ad}	adsorption-desorption frequency (s^{-1})
Z_{ad}	adsorption impedance (Ω)
$Z_d(\omega)$	diffusion impedance (Ω)
$Z_G(\omega)$	Gerischer impedance (Ω)
Z_G^o	resistance of Gerischer impedance (Ω)
$Z_F(\omega)$	finite-length Warburg impedance (Ω)
Z_F^o	resistance of finite-length Warburg impedance (Ω)

References

1. W. Vielstich, H.A. Gasteiger, A. Lamm, Handbook of Fuel Cells-

Fundamentals, Technology and Applications, John Wiley & Sons, New York, pp. 588-600 (2003).
2. J. Mizusaki, K. Amano, S. Yamauchi and K. Fueki, Solid State Ionics, **22**, 313 (1987).
3. J. Mizusaki, H. Tagawa, K. Tsuneyoshi and A. Sawata, J. Electrochem. Soc., **138**, 1867 (1991).
4. M. J. L. Ostergard and M. Mogensen, Electrochim. Acta, **38**, 2015 (1993).
5. A. M. Svensson, S. Sunde and K. Nisancioglu, Solid State Ionics, **86-88**, 1211 (1996).
6. Y. Matsuzaki and I. Yasuda, Solid State Ionics, **126**, 307 (1999).
7. G. W. Coffey, L. R. Pederson and P. C. Rieke, J. Electrochem. Soc., **150**, A1139 (2003).
8. X. J. Chen, K. A. Khor and S. H. Chan, Solid State Ionics, **167**, 379 (2004).
9. A. J. A. Winnubst, A. H. A. Scharenborg and A. J. Burggraaf, Solid State Ionics, **14**, 319 (1984).
10. B. Gharbage, T. Pagnier and A. Hammou, J. Electrochem. Soc., **141**, 2118 (1994).
11. R. Jimenez, T. Kloidt and M. Kleitz, J. Electrochem. Soc., **144**, 582 (1997).
12. N. Q. Minh, S. P. S. Badwal, M. J. Bannister, R. H. J. Hannink (Ed.), Science and Technology of Zirconia, Technomic Publishing Co., Lancaster, pp. 652-687 (1993).
13. N. Q. Minh, T. Takahashi, Science and Technology of Ceramic Fuel Cells, Elsevier Science B.V., Amsterdam, pp. 117-146 (1995).
14. E. Siebert, A. Hammouche and M. Kleitz, Electrochim. Acta, **40**, 1741 (1995).
15. K. Tsuneyoshi, K. Mori and A. Sawata, Solid State Ionics, **35**, 263 (1989).
16. X. J. Chen, K. A. Khor and S. H. Chan, J. Power Sources, **123**, 17 (2003).
17. M. J. Verkerk and A. J. Burggraaf, J. Electrochem. Soc., **130**, 78 (1983).
18. R. U. Atangulov and I. V. Murygin, Solid State Ionics, **67**, 9 (1994).
19. B. A. Boukamp, H. J. M. Bouwmeester, Solid State Ionics, **157**, 29 (2003).
20. J. Mizusaki, Y. Mima, S. Yamauchi, K. Fueki and H. Tagawa, J. Solid State Chem., **80**, 102 (1989).
21. S. P. Jiang, Solid State Ionics, **146**, 1 (2002).
22. S. B. Adler, J. A. Lane, B. C. H. Steele, J. Electrochem. Soc., **143**, 3554 (1996).
23. J.-S. Kim, S.-I. Pyun, J.-W. Lee and R.-H, Song, submitted to Electrochim. Acta for publication, (2005).
24. S. B. Adler, Chem. Rev., **104**, 4791 (2004).
25. J. Nowotny and M. Rekas, J. Am. Ceram. Soc., **81**, 67 (1998).
26. F. W. Poulsen, Solid State Ionics, **129**, 145 (2000).
27. T. Ioroi, T. Hara, Y. Uchimoto, Z. Ogumi and Z. Takehara, J. Electrochem. Soc., **145**, 1999 (1998).
28. S. P. Jiang and J. G. Love, Solid State Ionics, **138**, 183 (2001).
29. D. Braunshtein, D. S. Tannhauser and I. Riess, J. Electrochem. Soc., **128**, 82 (1981).
30. J. Sasaki, J. Mizusaki, S. Yamauchi and Kazuo Fueki, Bull. Chem. Soc. Jpn., **54**, 1688 (1981).
31. S.B. Adler, Solid State Ionics, **111**, 125 (1998).
32. S. P. Jiang, J. Power Sources, **124**, 390 (2003).